Distinct Seasonal Primary Production Patterns in the Sub-Polar Gyre and Surrounding Seas

Katherine Richardson[1][*][†] and Jørgen Bendtsen[2,3][†]

[1] Center for Macroecology, Evolution and Climate, Globe Institute, University of Copenhagen, Copenhagen, Denmark,
[2] Norwegian Institute for Water Research, NIVA Denmark, Copenhagen, Denmark, [3] ClimateLab, Copenhagen, Denmark

Primary production (PP) in the sub-polar region appears to be important for ocean carbon uptake but how the different water masses contribute to the PP occurring here has not yet been described. Using two models based on satellite observations of surface chlorophyll, light and temperature, seasonal patterns in the distribution of PP are shown here to differ in the sub-polar gyre south of the Greenland-Scotland Ridge (GSR) and surrounding water masses. Monthly averages of PP (2003–2013) were determined. Total and seasonal PP were similar in both models. Average PP in five of the domains (0.47–0.77 g C m^{-2} d^{-1}) was well above the global average (0.37 g C m^{-2} d^{-1}). Over the East Greenland shelf, however, total annual PP was estimated to be only 0.19 g C m^{-2} d^{-1}. The Norwegian shelf was the most productive of the regions studied. "Spring blooms" appear sporadically as spikes in the annual distribution of PP in some regions/years, but do not emerge as a dominant feature in the average annual development of PP in any of the domains. For all regions, ~25% of the annual PP takes place in the period January-May. PP peaked over most of the study area at or around maximum insolation or temperature. PP in the study region as a whole appears to be more related to latitude or water masses than to bathymetry. In waters over the East Greenland shelf, the Norwegian shelf, and north of the GSR up to 50% of annual PP had taken place when ~50% of the annual flux of light has reached the surface. In contrast, only about 35% of annual PP had taken place in the sub-polar gyre and waters over the southern open shelf by this time. Light-use efficiency differences may be explained by differences in mixed layer depth (MLD). Multi-model Earth System model studies have indicated that climate change may decrease the MLD in the sub-polar gyre and suggest this may lead to a decrease in the PP occurring here. The results presented here, however, suggest that a shallower MLD could lead to an increase in PP.

Keywords: spring bloom, North Atlantic, primary production, light, temperature, primary production model

INTRODUCTION

The waters in and surrounding the North Atlantic sub-polar gyre are recognized as being important in atmospheric CO_2 drawdown. Chemical-physical processes alone, however, cannot completely explain observed distribution patterns in surface water CO_2 (Takahashi et al., 2009) and it is therefore assumed that removal of CO_2 from surface waters by phytoplankton photosynthesis

[primary production (PP)] is an important driver in the development of the seasonal distribution of CO_2 in these waters (Takahashi et al., 2002). Nevertheless, a detailed understanding of the seasonal patterns in PP in different water masses found in this region is still lacking.

The region is large and characterized by varied bathymetric conditions with shelves along East Greenland, Norway and the shallow Greenland-Scotland Ridge (GSR) that separate the open sea areas in the Nordic Seas and the sub-polar Gyre. In addition, regional-scale currents affecting both nutrient distributions and stratification characteristics pass through the area. Several studies have suggested that PP characteristics of these different water masses may differ (e.g., Astthorsson et al., 2007) and inter-annual variability has been shown to correlate with the North Atlantic Oscillation, i.e., the principal mode explaining atmospheric variability in the region (e.g., Skogen et al., 2007; Henson et al., 2009; Harrison et al., 2013). Linkages between PP and water mass distributions are also indicated from the timing and distribution of phytoplankton blooms (Friedland et al., 2016), and differences in the timing of the spring bloom across the GSR have been explained by water mass characteristics, e.g., mixed layer depth (Zhai et al., 2012) or iron-depletion (Nielsdóttir et al., 2009).

Climate change scenarios show significant changes in the sub-polar North Atlantic by the end of the 21st century where reduction in sea ice cover, increased stratification and changes in water mass distributions will affect PP in the area. PP in the sub-polar gyre is expected to decrease significantly whereas PP in areas north of the GSR shows a mixed response (Laufkötter et al., 2015; Kwiatkowski et al., 2020). Predictions of PP are, however, associated with large uncertainties and a better understanding of local drivers for PP, e.g., light, nutrients, grazing and stratification, is required for making robust future assessments.

The aim of the current study is to examine seasonal distribution patterns in PP in the sub-polar gyre and adjacent waters and to relate these patterns to physical conditions. As there are insufficient *in situ* data to address this question, we employ models estimating PP from surface optical water characteristics remotely determined from satellite observation (chlorophyll, light and temperature). Satellite sensors can only provide direct observations from the surface layer of the ocean and PP is well known to also occur below the surface layer. Thus, the validity of the estimates resulting from the models converting surface ocean characteristics to PP is highly dependent upon the model's approach to estimating PP in the water column as a whole. We chose, therefore, two different model approaches for estimating PP, where the principle difference between the models is the strategies employed for estimating total water column PP.

In the first, the commonly employed VGPM model (vertically generalized production model; Behrenfeld and Falkowski, 1997), sub-surface PP is estimated based on statistical analyses of archived chlorophyll profiles. In the other, VPP (vertically integrated primary production model; Richardson and Bendtsen, 2019), a universal pattern in the vertical distribution of PP in relation to nutricline depth is used to estimate sub-surface PP. In the study area, the nutricline is generally located close to the surface (Garcia et al., 2010). Thus, we argue that most of the water

column PP will occur near the surface layer and can be accurately estimated from surface water characteristics.

Models estimating PP are also highly sensitive to the photosynthetic parameters used (Behrenfeld and Falkowski, 1997). The same (temperature sensitive) maximum rates of photosynthesis (P^B_{max}) are used in both model approaches employed here. The parameterization of P^B_{max} used in the models was that used in VGPM and, thus, not based on data collected in the study region. We, therefore, evaluate the global VGPM parameterization against measurements of P^B_{max}-values from the North Atlantic.

The study area is divided into six regions, representing open sea and shelf areas and seasonal PP is analyzed in relation to light, photosynthetic parameters and mixed layer depth. The study suggests that changes in water column stratification characteristics in the sub-polar gyre can be expected to change the seasonal distribution and magnitude of PP here. A reduction of sea-ice along the East Greenland shelf would likely lead to an increase in the PP occurring in that region.

MATERIALS AND METHODS

Calculation of Primary Production

Primary production is calculated from observations of surface fields of chlorophyll, sea surface temperature (SST), photosynthetically active radiation (PAR, i.e., the fraction of incident light between 400–700 nm at the ocean surface) and from climatology of nutrient concentrations in the upper ocean. Two PP-models, VPP and VGPM, are applied in the analysis. In the VGPM-model, PP estimates are based on surface fields and empirical relations of the vertical distribution of chlorophyll a (Behrenfeld and Falkowski, 1997). In the VPP-model (described in section "Modeling PP"), water column PP is estimated based on a calculation of PP in the upper 10 m of the surface layer and empirical relations of the total water column PP determined by the distribution of nutrients in the upper ocean (Richardson and Bendtsen, 2019). On a global scale, the geographical distribution of PP differs significantly between the two models (Richardson and Bendtsen, 2019) and this motivates the use of both models in this study. A comparison is made between the regional PP estimates from the two models and the VPP-model is applied in the subsequent analysis of seasonal PP in the area.

Satellite Observations and Nutricline Climatology

Satellite observations (MODIS data provided by NASA) were obtained from the Ocean Productivity site[1] where global fields (1/12° × 1/12° spherical grid) averaged for 8 day periods between 2003–2013 are applied as input to the PP-models. Satellite data included fields of SST, PAR, surface chlorophyll a (chl) and the diffuse attenuation coefficient in the 490 nm band. Nutrient concentrations are estimated from the monthly climatology of nitrate in the World Ocean Atlas (Garcia et al., 2010). The nutricline depth (DNO_3) is defined as the depth where the nitrate

---

[1]www.science.oregonstate.edu/ocean.productivity

concentration is 1 μmol kg^{-1} (found by linear interpolation of the vertical profile of nitrate).

Photosynthetic Parameters

Calculation of PP depends on the photosynthetic parameters P^B_{max} (in VGPM and VPP) and α^B (in VPP), representing the chlorophyll a normalized maximum rate of photosynthesis and the initial slope of the PE-curve [i.e., PP (P) vs. irradiance (E) describing the light-dependent photosynthesis], respectively. The VGPM-model applies a temperature dependent parameterization of P^B_{max} that varies between 1.1 μg C (μg chl h)$^{-1}$ at low temperatures and a maximum value at 20°C of ∼7 μg C (μg chl h)$^{-1}$ (Behrenfeld and Falkowski, 1997). Temperature-dependence represents both the physiological response in phytoplankton to temperature and correlation between temperature and the geographical variation of phytoplankton community composition. A global analysis showed relatively large scatter of P^B_{max} as a function of temperature and also a significant dependence on the characteristic size of the phytoplankton community (Richardson et al., 2016) and nutrient concentration (Richardson and Bendtsen, 2019). However, variation of P^B_{max} is relatively small in cold water (<5°C) where it typically varies between 1–3 μg C (μg chl h)$^{-1}$. We apply the same parameterization for P^B_{max}, suggested by Behrenfeld and Falkowski (1997), in the two models. The influence of P^B_{max} on PP is considered by comparing the applied parameterization with P^B_{max}-values obtained from PP-incubation experiments on water samples from the area. The value of α^B is applied in the VPP-model and it is parameterized in three nutricline depth intervals; (1) DNO_3 < 20 m, (2) 20–90 m and (3) >90 m, as (1) 3.57, (2) 2.68, and (3) 1.59 {10^{-2} [μg C (μg chl h μE m^{-2} s^{-1})$^{-1}$]}, respectively (Richardson and Bendtsen, 2019).

Modeling PP

Primary production is calculated from the VGPM-model where it depends on P^B_{max}, surface concentration of chlorophyll a, the daily PAR and the depth of the euphotic zone estimated from the surface concentration of chlorophyll a (Behrenfeld and Falkowski, 1997).

Primary production calculated in the VPP-model assumes that the surface production in the upper 10 m, i.e., the approximate depth range visible from satellites, can be related to the total PP via a relation to D_{NO3} (Richardson and Bendtsen, 2019). PP in the upper 10 m is calculated according to Webb et al. (1974):

$$PP_{10m} = \int_0^{24h} \int_{-10m}^{0} P^B_{max} chl(z)$$

$$\left(1 - \exp\left(-PAR(t,z)\frac{\alpha^B}{P^B_{max}}\right)\right) dzdt \qquad (1)$$

where t is time, z is the vertical coordinate, and chl(z) and PAR(t, z) represent the vertical distribution of chlorophyll and PAR, respectively. The vertical distribution of light is considered by calculating the light-attenuation coefficient from the satellite-derived attenuation coefficient at 490 nm, and the temporal variation of PAR is considered by integrating Eq.

(1) with a time step of one hour during a 24-hour period. In principle, the integrals in Eq. (1) provide the total PP if the inner integral is integrated to the bottom of the euphotic zone. However, variations in chlorophyll and the photosynthetic parameters are poorly known and cannot be directly inferred from satellite data and, therefore, it only integrates the upper 10 m visible from space.

Richardson and Bendtsen (2019) analyzed global in situ PP in the surface layer and showed a significant nutricline depth dependence of PP_{10m} and the total PP; PP_{10m} = γ PP, i.e., γ represents the fraction of total PP occurring in the upper 10 m. The fraction is defined in three nutricline depth intervals: (1) D_{NO3} less than 20 m, γ = 31.0%, (2) between 20 and 90 m, γ = 19.0%, and (3) deeper than 90 m, γ = 10.7%, respectively. This implies, for example, that only 10.7% of total PP takes place in the upper 10 m in oligotrophic areas where the nutricline depth is below 90 m depth, and that PP can be calculated as: PP = PP_{10m}/γ. Correspondingly, in areas with a shallow nutricline (i.e., $D_{NO3} \leq$ 20 m), as in the sub-polar region, a total of 31% of the vertically integrated PP is estimated to take place in the upper 10 m.
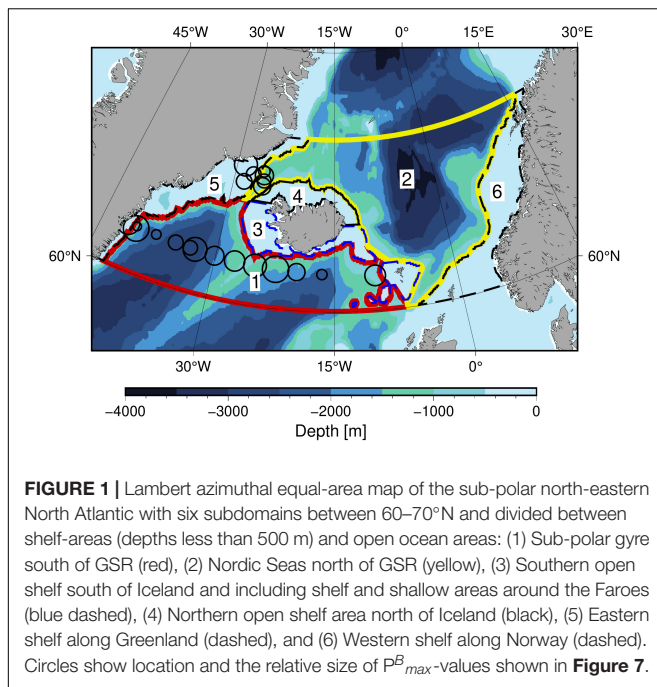
Measurements of Photosynthetic Parameters

Measurements of P^B_{max} in the study area were obtained from primary production incubation experiments from surface (5 m) water samples collected in August 2006 on the Galathea 3 expedition (on board R/V Vædderen) and from two cruises with R/V Dana in the North Atlantic in August 2008 and September 2012, respectively (Richardson and Bendtsen, 2019). Primary production was measured according to a modified carbon-14 method (Steemann Nielsen, 1952), and photosynthetic parameters were determined by fitting a PP vs. light intensity curve to data (Hilligsøe et al., 2011). Samples were collected south of the GSR along approximately 62.5°N from the East Greenland shelf and into the Iceland basin, and in an area north of the Denmark Strait at ∼67.5°N (**Figure 1**).

Mixed Layer Depth

We calculated mixed layer depth (MLD) from the climatology of de Boyer Montégut et al. (2004). The mixed layer depth was interpolated from the climatological 2° latitude by 2° longitude grid onto the 1/12° x 1/12° degree grid applied by the PP-models and monthly averaged values were calculated for each of the six domains. A comparison of several MLD-climatologies has shown that differences can be large where stratification is weak due to different MLD-detection algorithms and observational data sets (Holte et al., 2017). However, here we only apply the MLD-climatology for comparing the relative seasonal difference between the six areas.

Shelf and Open Sea Areas

Shelf areas in the Arctic are relatively wide and deep, with mean depths of more than 300 m (Paris et al., 2016), and are confined within the shelf break from where a relatively steep slope (∼> 3%, e.g., Heezen et al., 1959) leads to the bottom of the ocean basins.

FIGURE 1 | Lambert azimuthal equal-area map of the sub-polar north-eastern North Atlantic with six subdomains between 60–70°N and divided between shelf-areas (depths less than 500 m) and open ocean areas: (1) Sub-polar gyre south of GSR (red), (2) Nordic Seas north of GSR (yellow), (3) Southern open shelf south of Iceland and including shelf and shallow areas around the Faroes (blue dashed), (4) Northern open shelf area north of Iceland (black), (5) Eastern shelf along Greenland (dashed), and (6) Western shelf along Norway (dashed). Circles show location and the relative size of P^B_{max}-values shown in **Figure 7**.

We define the shelf area as being where the bottom depth is less than 500 m, i.e., containing the shallow continental shelf as well as deeper areas within, typically, ∼10 km of the 2–400 m iso-depth.

We consider the sub-polar area between 60–70°N (**Figure 1**), located between Greenland and Norway. We refer to the open sea areas south and north of the GSR and within the latitude limits as the sub-polar gyre and the Nordic Seas, respectively, although they geographically only cover part of these areas. Shelf area is shallower than 500 m, except for two deep (>500 m) and relatively narrow troughs across the East Greenland shelf (∼66°N) which are categorized as shelf areas.

Previous studies have shown that biological production differs in timing between the shelf north and south of Iceland (e.g., Zhai et al., 2012; Friedland et al., 2016), and this motivates the separation of the shelf area north of Iceland as a separate domain. Correspondingly, Friedland et al. (2016) showed that the entire shelf area around the Faroes (located south of Iceland) shares some similarity in terms of frequency and start of the spring bloom with conditions in the Iceland basin. Therefore, this area is considered together with the shelf south of Iceland. The sub-polar north-eastern North Atlantic is thereby divided into six subdomains representing either shelf or open sea areas; (1) Sub-polar Gyre south of GSR, (2) Nordic Seas north of GSR, (3) Southern open shelf south of Iceland and including shelf and shallow areas around the Faroes, (4) Northern open shelf area north of Iceland, (5) Eastern shelf along Greenland, and (6) Western shelf along Norway.

Statistical Tests

Comparison of average values from different domains and the two models are based on Welch modified two-sample t-test. Statistical p-values are calculated in R (R Core Team, 2021) using the BSDA-package (Arnholt and Evans, 2021) (low p-values indicate significantly different mean values). Correlations between time-series from different domains are calculated from Pearson's r (Press et al., 1992).

RESULTS

Annual PP in the Sub-Polar Region

The average global PP estimate in the period 2003–2013 by the VPP-model is 49 Pg C yr^{-1} (**Table 1**). This is comparable to the global PP of 48 Pg C yr^{-1} estimated by the VGPM model ($p < 0.004$). The spatial distribution of the averaged regional PP in the period 2003–2013 is shown in **Figure 2**. The largest annual PP (0.5–1 g C m^{-2} d^{-1}) is located in a belt around the GSR from Iceland toward the Faroes and along the Norwegian coast (**Figure 2A**). Slightly lower values (0.3–0.5 g C m^{-2} d^{-1}) characterize the southern part of the sub-polar subdomain in the Irminger Sea and parts of the Iceland basin. Similar values are found north of the GSR in the Nordic Seas with a gradual decrease toward the shelf along east Greenland. The associated standard deviations show that the largest variability of the annual PP ($\pm$ 0.3–0.5 g C m^{-2} d^{-1}) is seen above the shelf south of Iceland and in the southern part of the Norwegian shelf (**Figure 2B**). However, relatively large variability ($\pm$ 0.2–0.3 g C m^{-2} d^{-1}) is also seen north and south of the Faroe Islands and above the Reykjanes ridge (the Reykjanes ridge is shown in **Figure 1** as the shallow area directly southwest of Iceland).

The corresponding PP estimated by the VGPM-model shows a similar distribution in the study area. The ratio of the VPP and the VGPM-estimates indicates higher PP estimated by the VPP-model along the GSR and south of the Faroes, whereas there is a tendency toward a lower production in the southern part of the sub-polar domain and northern part of the Nordic Seas, respectively (**Figure 2C**). The difference between the two estimates is, however, relatively small and VGPM-values averaged in the six areas (not shown) is only 1–12% lower than in the VPP-model (differences are only significant in area 3, 4, and 6 where $p < 0.05$). In total, the study area in the sub-polar region covers an area of $2.4 \cdot 10^{12}$ m^2 and accounts for an annual averaged PP of 0.46 Pg C yr^{-1}, i.e., an average production of 0.53 g C m^{-2} d^{-1} (**Table 1**).

PP Above Shelves vs. Open Ocean

Shelf areas, i.e., domains 3–6, cover a total area of $0.70 \cdot 10^{12}$ m^2, corresponding to 29% of the area in the study region (domains 1–6). The corresponding PP above the shelves accounts for 0.15 Pg C yr^{-1}, or 32% of PP in the area (**Table 1**). Thus, the area-normalized PP from shelf areas, in general, approximately corresponds to the average PP in the area. However, PP above the shelves spans a relatively large interval from the low values along east Greenland of 0.19 g C m^{-2} d^{-1} to the highest value along the Norwegian coast of 0.77 g C m^{-2} d^{-1}. The annual average PP above the southern shelves in the sub-polar gyre of 0.72 g C m^{-2} d^{-1} was higher than that estimated for the surrounding open sea ($p < 1e-6$). Similarly, production along the shelves north of Iceland and along the Norwegian coast was

TABLE 1 | Annual average PP calculated by the VPP-model, for the period 2003–2013, for the global domain (domain no. 0) and for the six subdomains in the northern North Atlantic (domain 1–6).

Domain	Area	VPP	VPP	VPP(spring)	$\frac{VPP(spring)}{VPP}$
No.	10^{12} m^2	Pg C yr^{-1}	g C m^2 d^{-1}	Pg C yr^{-1}	%
0 (global)	361.9	49.1 ± 1.1	0.37 ± 0.01	–	–
1 (Sub-polar gyre)	0.747	0.15 ± 0.02	0.53 ± 0.06	0.031 ± 0.004	21
2 (Nordic Seas)	0.930	0.16 ± 0.02	0.47 ± 0.05	0.042 ± 0.007	26
3 (Southern shelves)	0.167	0.044 ± 0.003	0.72 ± 0.05	0.010 ± 0.001	22
4 (Shelf north of Iceland)	0.082	0.016 ± 0.002	0.55 ± 0.06	0.004 ± 0.001	27
5 (Shelf along East Greenland)	0.186	0.013 ± 0.003	0.19 ± 0.04	0.002 ± 0.001	12
6 (Shelf along Norway)	0.262	0.074 ± 0.008	0.77 ± 0.08	0.025 ± 0.003	34

Values of the areas in each domain, the total VPP, the corresponding VPP per area, the VPP(spring), i.e., PP from 1st of January to 1st of June, and the ratio between PP(spring) and the annual PP (values shown with standard deviations).

higher than in the Nordic Seas ($p < 0.004$). Thus, shelf PP is greater than in the ambient open sea in the region, except for the shelf along East Greenland.

Contribution of Spring PP to Annual PP

Dramatic peaks in chlorophyll concentration are commonly observed in surface waters during spring in temperate regions (e.g., Henson et al., 2009) and these "blooms" are often assumed to constitute an important signal in the annual PP cycle. As the timing of these blooms differs inter-annually, we examine the contribution of PP over the first 5 months of the year to total annual PP. If the spring bloom makes a disproportionally large contribution to annual PP, we would expect to find a disproportionally large PP during these months. Thus, we estimate "spring" PP by estimating total PP from 1 January – 1 June and by comparing PP during this five-month period to the annual PP, i.e., VPP(spring)/VPP (**Table 1**).

Primary production during the first 5 months of the year contributes with between 12 and 34% of the annual PP in the six domains. The largest contribution of this spring to total PP is seen along the Norwegian shelf, despite the fact that a significant fraction of this shelf area is located at high latitudes (**Table 1**). It is noteworthy that PP during the first 5 months of the year contributes a smaller fraction of the annual PP in the sub-polar gyre south of the GSR (21%) than it does in the Nordic Seas (26%, $p < 0.02$).

Differences in PP could arise from different light conditions between the northern and southern parts of the study area. The accumulated insolation (at the top of the atmosphere) from 1 January–1 June at 70°N [corresponding to an average flux of $\sim$168 W m^{-2} during the 5 month period, calculated from a global insolation climatology (Hartmann, 1994)] is about 22% less than insolation at 60°N ($\sim$217 W m^{-2}). The fractions of insolation occurring during the 5 month period compared to the annual insolation are 36 and 38% at the two latitudes, respectively. Thus, despite open sea areas north of the GSR receiving relatively less insolation during the spring period, they have a higher percentage of total annual PP occurring during the spring than in the open sea area south of the GSR. The average spring PP per unit area of 0.29 g C m^{-2} in the Nordic Seas is also slightly (not significantly) larger than in the sub-polar gyre (0.27 g C m^{-2} d^{-1}). Together,

these results suggest that open sea spring PP south of the GSR is more limited by factors other than light, e.g., mixed layer depth, nutrients or grazing, than is the case north of the GSR.
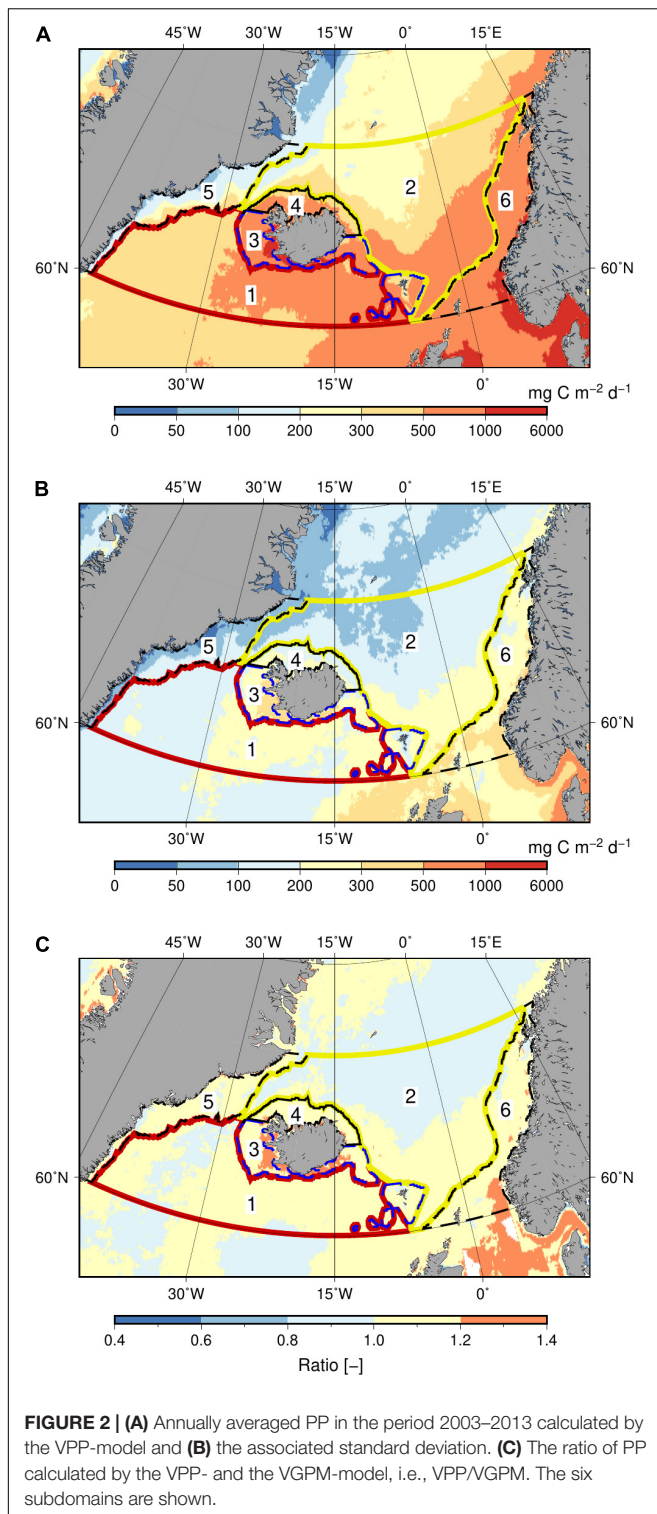
A similar pattern is noted with respect to shelf sea areas as PP during the first 5 months of the year over the open shelf south of the GSR contributes less (22%) to the annual PP than the open shelf north of the GSR (27%, $p < 0.02$) (**Table 1**). The shelf along east Greenland shows the lowest spring contribution (12%) to annual PP. This can partly be explained by the extensive sea ice cover until early summer along the northern part of the shelf. Relatively high spring production along the ice-free Norwegian shelf contributes with about a third of the annual production (34%). Thus, this domain experiences a significantly more productive spring period than is seen along East Greenland at the western boundary of the basin.
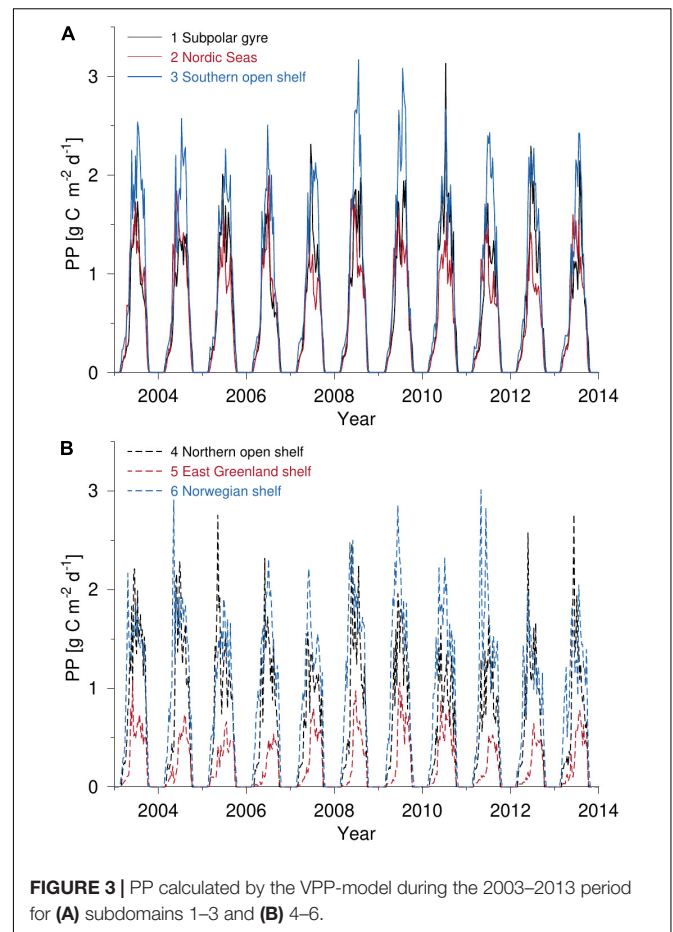
Inter-Annual Variability

Inter-annual variability of PP in the sub-polar area is clearly seen by comparing peak values of PP during the 2003–2013 period, e.g., variations between 2.3–3.1 g C m^{-2} d^{-1} at the southern open shelf or 0.5–1.1 g C m^{-2} d^{-1} along East Greenland (**Figure 3**). Time series from the different subdomains also show that the timing of the initial peak in PP varies significantly from year to year, and that some years are characterized by a relatively strong spring bloom PP signal which is not present in other years. For example, production in 2005 over the northern open shelf shows peak values above 2.8 g C m^{-2} d^{-1} whereas PP in 2007 remains below 1.6 g C m^{-2} d^{-1}. There is also a large inter-annual variation in the structure of the seasonal PP. Some years are characterized by a single peak of PP during spring or summer and a modest production the rest of the growth season, e.g., the sub-polar gyre in 2007, while other years are characterized by an initial bloom followed by a bloom later in the season, e.g., the southern open shelf in 2009 or the Norwegian shelf in 2011. Comparison of PP above the Norwegian shelf and along East Greenland shows how sea ice delays production but also that PP is significantly lower along east Greenland than elsewhere in the sub-polar area.

Seasonal PP

The largest monthly averaged PP between 2003–2013 takes place above the southern open shelf in July and about a month

FIGURE 2 | **(A)** Annually averaged PP in the period 2003–2013 calculated by the VPP-model and **(B)** the associated standard deviation. **(C)** The ratio of PP calculated by the VPP- and the VGPM-model, i.e., VPP/VGPM. The six subdomains are shown.

FIGURE 3 | PP calculated by the VPP-model during the 2003–2013 period for **(A)** subdomains 1–3 and **(B)** 4–6.

PP above the Norwegian shelf than for the southern open shelf (0.77 and 0.72 g C m^{-2} d^{-1} for the Norwegian and southern open shelves, respectively: **Table 1**). The East Greenland shelf shows an asymmetric seasonal PP distribution pattern with a maximum in July and relatively low area-averaged production. The Nordic Seas, the northern open shelf and the sub-polar gyre all exhibit maximum PP during June, i.e., coincident with maximum insolation. The largest increase in PP is seen in the Nordic Seas and the northern open shelf during April and May, whereas a longer and steady increase characterizes the sub-polar gyre between April and June.

The seasonal evolution of PP estimated by the VGPM model (**Figure 4**) shows qualitatively similar results as the VPP-model (not shown). The largest difference is between the peak July value above the Southern open shelf where the VPP estimates 2.18 g C m^{-2} d^{-1} as opposed to 1.84 g C m^{-2} d^{-1} in the VGPM-model, corresponding to a difference of 16%. Otherwise, the models yield similar results and show only minor differences in the seasonal dynamics, i.e., similar shape and timing of peak PP values. In addition, the absolute values of the monthly averages for the 11-year period are in good accordance. In general, the VPP model PP estimate is 5–15% higher than the VGPM model in the period from April-September.

later than maximum insolation occurs (**Figure 4**). Production above the Norwegian shelf shows similarly high values but also a longer growth season extending from March to September and more closely following the seasonal change in insolation. This may explain the slightly (not significant) higher annual
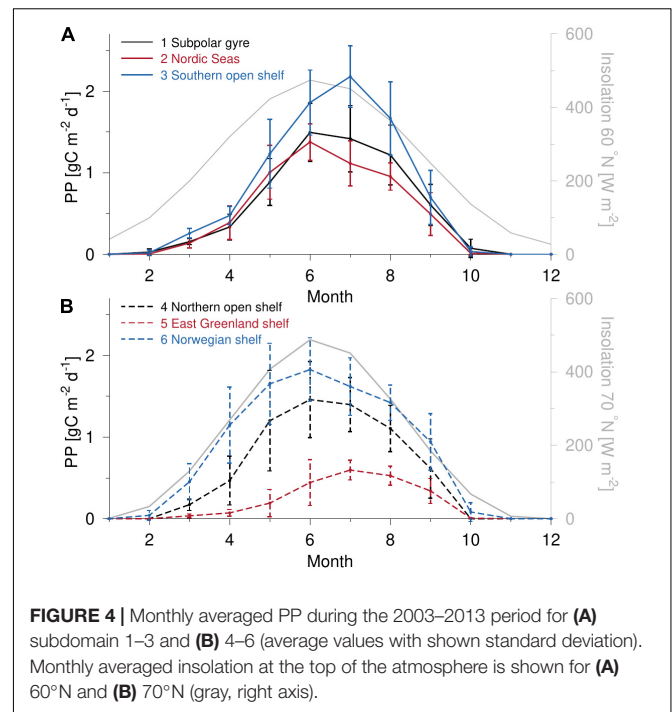
Seasonal PAR and Chlorophyll

Seasonal PAR in the six areas is mainly driven by the latitudinal distribution between 60–70°N where, for example, the sub-polar gyre receives ∼10% more light than the Nordic Seas from May to July due to its being located at lower latitudes (**Figure 5A**). However, there are some significant differences among the shelf areas. Surface water above the east Greenland shelf is largely covered by sea ice in early spring. Monthly averaged ice cover is about 70% until May, decreasing to 53% in June and the sea ice minimum is first achieved in August (ice cover < 5%). This results in very low area-averaged PAR being received by the East Greenland shelf water in spring and until June and explains the low area-averaged PP in this area (**Figure 4B**). Another difference, which cannot be explained by latitude, is seen between the slightly lower PAR received in the sub-polar gyre than above the Norwegian shelf during spring and summer. Although most of the Norwegian shelf is located at higher latitudes than the sub-polar gyre, the tendency of less cloudiness during spring and summer above the Norwegian shelf results in a more illuminated environment.

The seasonal distribution of chlorophyll in the sub-polar gyre and in the Nordic Seas (**Figure 5C**) resembles the seasonal PP-distribution (**Figure 4**), with a tendency for slightly higher chlorophyll concentrations during spring in the Nordic Seas, which is also reflected in the spring PP-distributions here. Chlorophyll concentrations above the southern open shelf achieve a relatively large maximum in July and this explains the resultant large PP in this area. Low area-averaged chlorophyll values above the east Greenland shelf, due to the large extent of sea ice cover, are also in accordance with the low seasonal PP here. However, the chlorophyll distributions over the Norwegian shelf and in the northern open sea shelf are significantly different from their seasonal PP-distributions, where monthly averaged chlorophyll shows a relatively large spring peak in the two areas (**Figure 5C**) while the PP distribution only shows a gradual increase during spring and early summer (**Figure 4B**). This implies that other factors than chlorophyll concentration are important for explaining the estimated PP in these two areas.

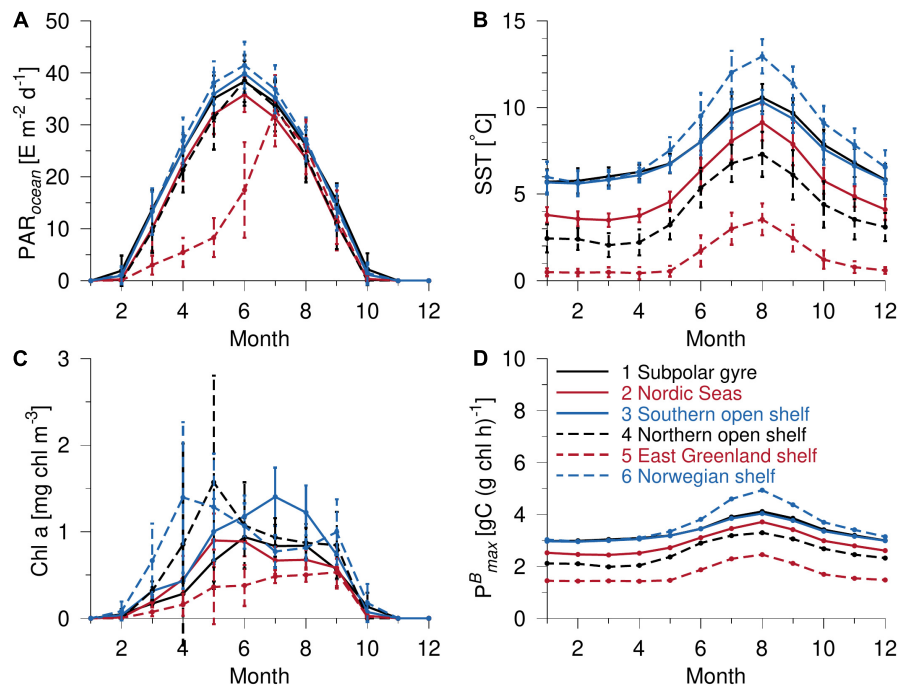## Photosynthetic Parameters and Sea Surface Temperature

In addition to light and chlorophyll concentration, PP depends on the photosynthetic parameters P^B_{max} and α^B (i.e., dependent upon D_{NO3} in the VPP-model). Both the VPP and VGPM models apply the SST-dependent parameterization of P^B_{max} developed by Behrenfeld and Falkowski (1997), and the relatively large SST increase during summer in the six areas (**Figure 5B**) thus implies a corresponding increase in P^B_{max} (**Figure 5D**). The large SST increase above the Norwegian shelf from 5.9°C in March to 13.0°C in August results in a corresponding increase of P^B_{max} from 3.0 to 4.9 μg C (μg chl h) $^{-1}$, i.e., an increase of more than 60%. This implies a correspondingly higher estimate of PP during summer in both models. The onset of the seasonal thermocline is seen to have a similar significant impact where P^B_{max} increases accordingly in all six areas.
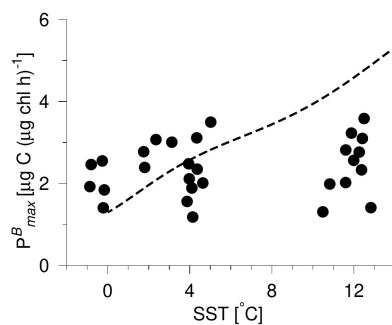

FIGURE 4 | Monthly averaged PP during the 2003–2013 period for **(A)** subdomain 1–3 and **(B)** 4–6 (average values with shown standard deviation). Monthly averaged insolation at the top of the atmosphere is shown for **(A)** 60°N and **(B)** 70°N (gray, right axis).

The SST-dependent parameterization of P^B_{max} was assessed by comparing directly with measurements from the study area (**Figure 6** and **Supplementary Material**). The applied parameterization of P^B_{max} increased from 1.3 to 5 μg C (μg chl h)$^{-1}$ in the SST range between 0 and 13°C whereas measurements showed a more narrow range of 1.2–3.6 μg C (μg chl h)$^{-1}$ and there was no significant increase with temperature (**Figure 6**, dashed line and bullets, respectively). The average value of the measured P^B_{max}-values was 2.4 ± 0.7 μg C (μg chl h)$^{-1}$ (n = 21).

Spatial Correlation of PP

The annual production shows the largest PP above shelf areas, except for the east Greenland shelf. Interaction between shelf and open sea areas was therefore investigated by analyzing the correlation of PP during the growth season from the six domains during the 11-year period (**Table 2**, n = 294–327 for each of the six areas). In general, PP between all the areas is closely correlated because of the PP relationship to seasonal insolation. However, the largest correlation is seen between the sub-polar gyre and the open southern shelf, and between the Nordic Seas and the Norwegian shelf (Pearson's r of 0.91 and 0.88, respectively). This indicates that PP in the sub-polar area is more related to latitude or water masses than to bathymetry. This is also in accordance with conditions at the northern open shelf where the largest, although somehow lower (r = 0.82), correlation is with the Nordic Seas. The east Greenland shelf shows only a relatively weak correlation to the other domains, and the highest correlation is with the open southern shelf and the sub-polar gyre (r = 0.79 and 0.77, respectively) indicating that the correlation is mainly driven by ice-free conditions during spring and early summer in the southern part of this domain.

FIGURE 5 | Monthly averaged values (with standard deviation) for the six subdomains in the 2003–2013 period for **(A)** PAR, **(B)** SST, **(C)** chlorophyll a, and **(D)** P^B_{max}.

FIGURE 6 | Calculated P^B_{max} from incubation experiments versus SST (bullets, water samples are from the surface (5 m) and locations are shown in **Figure 1**), and the applied parameterization of P^B_{max} in the VPP and VGPM-models (dashed line).

Light Limitation and PP

The relative influence of light limitation in the six domains was analyzed (**Figure 7**) from the accumulated (acc) monthly (i = 1–12) area-averaged values of PAR_{acc} (μE m^{-2}) and PP_{acc} (g C m^{-2}), respectively, e.g., calculation of PP_{acc} becomes:

$$PP_{acc}(i) = \sum_{m=1}^{i} PP(m)\, \Delta t(m) \qquad (2)$$

where PP(m) and Δt(m) are the monthly averaged PP (g C m^{-2} d^{-1}) and the time (number of days) in each month, respectively. The accumulated PP and PAR for each month are
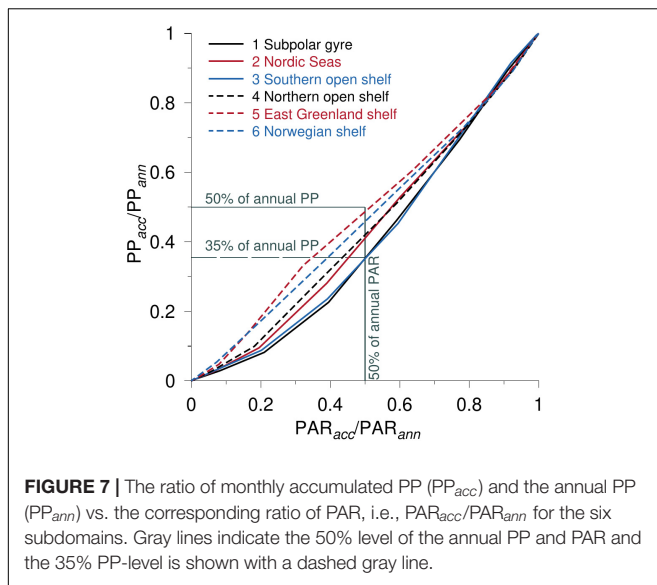
normalized with the accumulated annual PP (PP_{ann}, i = 12) and PAR, respectively, i.e., $PP_{acc}(i)/PP_{ann}$ and $PAR_{acc}(i)/PAR_{ann}$. The relationship between these two ratios shows the relative response of accumulated PP to the accumulated PAR. For example, if the accumulated PP is 50% when the area has received 50% of the annual PAR, then phytoplankton is equally effective in using light for PP before and after the time when half of the annual PAR has reached the water surface. Analyzing accumulated PP in relation to the accumulated PAR also considers asymmetries between areas due to sea ice cover or seasonal variability in cloudiness, e.g., the accumulated PP in ice-covered regions can be related to the received accumulated PAR in the water rather than insolation above the (ice-covered) surface.

The relative largest impact from light on PP is seen above the east Greenland shelf where ~50% of the annual PP is produced when the area has received ~50% of the annual PAR (**Figure 7**). Thus, while the area receives a relatively small amount

TABLE 2 | Correlation matrix (Pearson's r) between PP in the six subdomains and for the period 2003–2013 (n = 294–327, all are significant).

Domain no.	2	3	4	5	6
1	0.82	0.91*	0.67	0.77	0.71
2		0.86	0.82*	0.66	0.88*
3			0.78	0.79*	0.75
4				0.56	0.64
5					0.55

The largest correlation for each subdomain is indicated with an asterisk.

FIGURE 7 | The ratio of monthly accumulated PP (PP_{acc}) and the annual PP (PP_{ann}) vs. the corresponding ratio of PAR, i.e., PAR_{acc}/PAR_{ann} for the six subdomains. Gray lines indicate the 50% level of the annual PP and PAR and the 35% PP-level is shown with a dashed gray line.

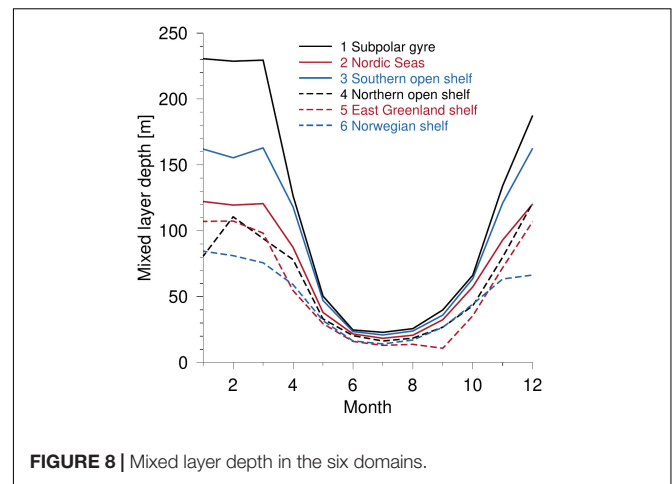**FIGURE 8 |** Mixed layer depth in the six domains.

of insolation during the season due to sea ice cover and the high latitudes, phytoplankton efficiently utilize light when it becomes available. Production above the Norwegian shelf is seen to be almost as efficient in terms of light usage. In general, photosynthesis in areas north of the GSR is significantly more effective in using light early in the season than areas south of the GSR, i.e., the sub-polar gyre and the Southern open shelf have only produced ~35% of the annual production when the areas have received ~50% of the annual PAR. Thus, phytoplankton in these domains have a relatively less efficient use of light during spring than later in the year.

Seasonal MLD

The deepest mixed layers in the study area are located south of the GSR where MLD in the sub-polar gyre and the southern open shelf area reaches 230 and 160 m during winter, respectively, whereas MLDs were less than 125 m for the other domains (**Figure 8**). Thus, the sub-polar gyre and the southern open shelf have relatively deep mixed layers in the start of spring, and it remains deeper in these domains with respect to the other areas during the rest of the year. MLD from June to August is less than 25 m in the entire study area and, from September, MLD increases in all areas.

DISCUSSION

The results presented here demonstrate differences in the seasonal distribution of PP in the sub-polar gyre and surrounding waters. PP peaks in all regions during summer. When data for the 11-year study period are averaged, the PP occurring during the first 5 months of the year does not make a disproportionally large contribution to annual PP in any of the regions. This suggests that spring blooms do not consistently constitute a significant signal in the annual PP occurring in this region. In the sub-polar gyre and southern open ocean (domains 1 and 3), phytoplankton

appear to use available light less efficiently during the spring period than in the more northerly domains.

PP in the Northern North Atlantic

Both total PP per unit area and its seasonal distribution patterns are shown to differ in the different sub-polar water masses studied here. Results from the VPP-model are compared with estimates from the VGPM-model which has been applied in previous model-intercomparison studies (e.g., Carr et al., 2006). Estimates from the two PP-models show a similar pattern with elevated annual PP along the GSR and the Norwegian shelf and low values above the East Greenland shelf. The models employed differ mainly in the treatment of light in the upper ocean and, for the VPP-model, a dependence on nutricline depth. However, nutricline depth levels in this region are generally shallow during the growth season, i.e., less than 20 m (except for a narrow band along the Norwegian coast from July–September where $D_{NO3} < 30$ m). Thus, the nutricline-dependence of photosynthetic parameters in the VPP-model does not contribute significantly to the spatial variability.

The total annual PP in the northern North Atlantic between 60 – 70°N is estimated to 0.46 Pg C yr^{-1}. Although this value is only about 1% of total global annual production (~49 Pg C yr^{-1}), the area-averaged sub-polar PP of 0.53 g C m^{-2} d^{-1} is ~42% larger than the global averaged value (0.37 g C m^{-2} d^{-1}). In addition to supplying ecosystems with energy in the form of organic carbon, PP also impacts the ocean carbon uptake. Several studies from individual years and smaller geographical areas have indicated that a peak in PP associated with a spring bloom appears as a dominant signal in the PP pattern (e.g., Zhai et al., 2012). In this study, however, where data (**Figure 3**) are averaged over the 11-year study period, it is shown that the PP occurring in the first 5 months of the year does not make a disproportionally large contribution to annual PP. Thus, spring blooms do not appear to be contributing with a dominant signal in the annual PP patterns in any of the six domains. The parameterized temperature dependence of P^B_{max} would tend to increase PP when SST increases (**Figure 5D**), thereby causing an increase of PP during the warmest period. We argue, however,

that the seasonal PP pattern found here is not a model artifact caused by the temperature dependence of P^B_{max}, as chlorophyll distributions also tend to peak during summer. In addition, we note that a similar seasonal pattern was reported based on PP estimates made from empirical data collected in the coastal waters around Denmark (Lyngsgaard et al., 2017).

Comparison With Measurements

Nevertheless, we compared the P^B_{max} values generated and applied in the models with measured P^B_{max}-values from the area. No significant dependence of P^B_{max} on SST was found for the *in situ* measurements, suggesting that the applied parameterization of P^B_{max} may overestimate PP during the warmest period (**Figure 6**). The parameterized P^B_{max} of 5 μg C (μg chl h) $^{-1}$ at an SST of 13°C is about a factor of two larger than the average value of measured P^B_{max}-values from the area. This implies that the absolute magnitude of PP estimated during summer may be higher than the actual, but it would not change the general shape of the seasonal distribution PP curve generated. Applying a smaller value during the warmest period would tend to increase the relative contribution of estimated PP during spring and, therefore, the estimated ∼25% of the annual PP occurring in the five-month period from 1 January to 1 June may be a low estimate. The spatial and temporal distributions of photosynthetic parameters, i.e., P^B_{max}, are therefore critical aspects to consider when the seasonal PP are evaluated from various PP-models covering the sub-polar region.

Comparison of PP estimated from the VPP-model and values obtained from measurements generally show good accordance in the six domains. Astthorsson et al. (2007) found that the annual PP above the southern open shelf (∼200–300 g C m^{-2} yr^{-1}) was significantly higher than at the shelf north of Iceland (100–200 g C m^{-2} yr^{-1}). This agrees well with the model estimates of the spatial gradients and the annual PP (263 ± 18 and 201 ± 18 g C m^{-2} yr^{-1} for the two areas, respectively: **Table 1**). Relatively high PP estimates (201 g C m^{-2} yr^{-1}, Debes et al., 2008) have also been reported over the shelf around the Faroe Islands. These estimates from the southern and northern open shelf areas are in general accordance with the VPP-estimates. Sanders et al. (2005) estimated the annual new production, i.e., that based on exogenous nutrient input (Dugdale and Goering, 1967), in the Irminger basin located between Greenland and Iceland (in the sub-polar domain) as 36 g C m^{-2} yr^{-1} based on nutrient measurements and satellite data. Similarly, Henson et al. (2006) estimated new production to 60 g C m^{-2} yr^{-1} based on satellite derived silicate distributions. New production is only a fraction of PP and is, thus, a lower bound of PP, and these estimates of new production are also significantly lower than our estimates of PP (100–200 g C m^{-2} yr^{-1}) in the Irminger Sea.

Harrison et al. (2013) estimated PP in the Norwegian Sea, located between the Norwegian shelf and the Greenland Sea, to be 80–120 g C m^{-2} yr^{-1}. This is in general agreement with our estimates of between 100–200 g C m^{-2} yr^{-1} for the area (**Figure 2A**). Zhai et al. (2012) analyzed the annual PP at six locations around Iceland by using satellite data and a vertically resolved model for calculating PP, and comparison with *in situ* measurements indicated that their estimated PP from remotely

sensed data were 50% too high. Their estimates of annual PP on the shelves north and south of Iceland showed a similar tendency to a higher production south of Iceland and their values were ∼25% larger for these locations than the corresponding estimates from the VPP-model (**Table 1**). Similarly, their locations in the Icelandic basin and Nordic Seas were in general agreement and ∼25% larger than the VPP-model.

Thus, the simple approach behind the VPP- and VGPM-models, where surface fields of chlorophyll a are the major factor for estimating PP, may represent the general distribution of PP but also lead to significant model-bias when compared to *in situ* measurements [see for example discussion in: Carr et al. (2006); Henson et al. (2006); Richardson et al. (2016)]. Local effects, not included in the models, may be important for PP. For example, the VPP-model considers the depth of the nutricline based on nitrate distributions, which has been shown to determine the fraction of PP occurring below the surface layer in large areas of the ocean (Richardson and Bendtsen, 2019). However, other nutrients are known to be important in the sub-polar area, e.g., silicate (Hátún et al., 2017) and iron (Nielsdóttir et al., 2009), and such limitations are not included in the PP-models used here.

Limitations due to local effects and the simple parameterizations of photosynthetic parameters will impact the absolute values of PP and also the seasonal variation in PP. However, the PP-models used here are mainly driven by the distribution of chlorophyll, and because the mixed layer depth (**Figure 8**) and nutricline depth are relatively shallow during the growth season in the sub-polar area, a significant fraction of total PP is estimated to take place in the upper 10 m. This is within the depth range where chlorophyll can be observed by satellites. Thus, we argue that the differences between the relative distributions found for the six domains are real, and that the different PP-levels between areas north and south of the GSR as well as between shelves and open sea areas reflect the spatial and temporal response of PP to the varying light and nutrient conditions in the sub-polar region.

Production Above Shelf Areas

On average, the shelf region in our study area contributes with a similar amount of PP per unit area as to the annual areal PP in the ambient open sea areas. However, the annual PP above the shelves spans a large interval with the least productive area being found above the east Greenland shelf (0.19 g C m^{-2} d^{-1}) and the most productive above the Norwegian shelf (0.77 g C m^{-2} d^{-1}). Thus, with the exception of the east Greenland shelf, the shelves are characterized by having the greatest area-averaged PP in the study area (**Table 1**). PP above these shelf areas is also characterized by relatively high PP and chlorophyll levels during spring (above the open northern shelf and the Norwegian shelf) and summer (the southern open shelf) where PP can reach values more than 50% higher than those occurring in the ambient open sea (**Figure 3**). Shelf areas are also characterized by a relatively large inter-annual variability where seasonal amplitudes can vary by more than 50% (e.g., large difference above the Norwegian shelf during spring between 2004 and 2005).

Correlation analysis of the 11-year time series of PP between the six areas shows that the greatest correlation is between

neighboring areas. Thus, production above the shelf areas is more closely related to the neighboring open sea areas than other shelf areas in the northern North Atlantic. This indicates that water masses are more important for the seasonal distribution of PP than processes related to differences between shelf-open sea dynamics, e.g., mixing processes. However, shelf areas are characterized by significantly larger PP than the ambient open sea area, e.g., the annual area-averaged PP above the southern open shelf ($0.72 \, \mathrm{g\,C\,m^{-2}\,d^{-1}}$) is 36% larger than in the sub-polar gyre.

Sub-Polar North-South Gradients in PP

When sub-polar areas have received 50% of the annual insolation in June, the east Greenland and Norwegian shelves and the open sea and shelf area north of GSR have produced 40–50% of their annual PP. The phytoplankton in these domains use light efficiently for photosynthesis during spring and early summer, whereas the sub-polar gyre and the southern open shelf only have produced about 35% of the annual PP in June (**Figure 7**). This implies that ∼65% of the annual PP takes place in the remaining part of the growth season where the area only receives 50% of the annual light. Thus, light harvesting by phytoplankton in the southern areas appears to be more efficient late in the summer season than during the spring. Although shelf production above the southern shelf is significantly greater than in the sub-polar gyre (**Table 1**), the similar low efficiency in light harvesting and the close correlation of PP between these areas indicate common limiting factors during spring and early summer.

The seasonal PP was analyzed at six locations around Iceland by Zhai et al. (2012) and they explained the later onset of PP south of Iceland as being due to a deeper mixed layer in spring and early summer. According to Sverdrup's critical depth hypothesis (Sverdrup, 1953), a net growth of phytoplankton biomass can first occur when the vertically integrated (light-limited) PP exceeds the respiratory losses in the mixed layer. Thus, a decreased MLD tends to increase PP because more biomass is in a more illuminated environment. We, therefore, analyzed the potential impact of MLD on PP in our study area by calculating the seasonal evolution of MLD in the six domains.

The deepest mixed layers in the study area are located south of the GSR where MLD in the sub-polar gyre and the southern shelf reaches 230 and 160 m during winter, respectively. MLDs were less than 140 m for the other domains (**Figure 8**). The sub-polar gyre and the southern open shelf have relatively deep mixed layers at the start of spring, and they remain deeper than MLDs in the other domains during the rest of the year. The relatively inefficient use of light in the sub-polar gyre and the open southern shelf during spring, manifested as a weak slope of the corresponding normalized PP-curves vs. light until June in **Figure 7**, occurs therefore at a time when these domains are characterized by a relatively deep mixed layer. The relatively deep MLD south of the GSR in spring may, therefore, explain the apparent reduced efficiency of light in PP here than in the other domains examined.

Analysis of bloom frequency and start days of blooms in the northern North Atlantic shows that blooms are more frequent in areas north of Iceland and that they, in general, start earlier in the season (Friedland et al., 2016), e.g., spring blooms are frequently seen from late April-May on the shelf north of Iceland whereas the less frequent blooms on the shelf south of Iceland typically start in May-June. This pattern is consistent with the spring peak seen in the seasonal chlorophyll distribution at the northern open shelf area and to a lesser extent in the Nordic Sea domain (**Figure 5C**).

Primary production over the shelf north of Iceland has been shown to correlate with salinity, i.e., PP tends to increase when saline Atlantic water is present (Astthorsson et al., 2007). Variability in water masses and winter convection and the extent of the sub-polar gyre south of Iceland have similarly been shown to explain productivity, biomass and nutrient distributions in the eastern sub-polar gyre (Hátún et al., 2016). Thus, PP in the sub-polar area is impacted by regional scale variability of water mass distributions and their influence on temperature, stratification and nutrients. In addition to the presence of macronutrients, the relatively low concentration of iron in the sub-polar gyre (Nielsdóttir et al., 2009) has been suggested to explain reduced photosynthetic efficiency during the growth season (Ryan-Keogh et al., 2013). The VPP-model only considers nitrate as a limiting nutrient, and nitrate only has a minor influence on the PP-estimates in the study area, so the influence from silicate (Hátún et al., 2017), iron or other limiting substances is not taken into account. In summary, several factors, in addition to MLD, may impact the seasonal PP and explain the seasonal difference in PP between areas on either side of the GSR.

Climate Change and Sub-Polar PP

The sub-polar North Atlantic plays a key role in the climate system where warm and saline subtropical water in the North Atlantic Current is transported into the area and continues toward the Nordic Seas or recirculates and mixes with upper water masses in the sub-polar gyre. This regional circulation constitutes the northern part of the Atlantic Meridional Overturning Circulation (AMOC) and, although transports in the sub-polar gyre and in the North Atlantic Current are not directly coupled (Lozier et al., 2010), they both have a major impact on transport of heat, salt and nutrients. Variability in circulation regimes of the sub-polar gyre therefore directly impacts nutrient concentrations and, thereby, productivity and ecosystem processes in the region (e.g., Hátún et al., 2016, 2017). Thus, large scale changes in circulation patterns in the North Atlantic are expected to impact PP in the sub-polar region. Circulation changes may also affect the relatively strong sink of atmospheric CO_2 in the sub-polar area (Takahashi et al., 2009). Biological production causes a significant drawdown of surface pCO_2 during the growth season and thereby enhances ocean carbon uptake in the area (Takahashi et al., 2002). Thus, feedback between PP and ocean carbon uptake may, in turn, affect global greenhouse gas concentrations.

The combined effect from these physical and biogeochemical changes on PP in the sub-polar area has been simulated in global circulation models. Kwiatkowski et al. (2020) analyzed a multi-model ensemble of Earth System Model (ESM) simulations under CMIP6 and found that PP on a global scale decreased between

0.6 ± 2.5% and 3 ± 9% by year 2100 in two climate change scenarios (a low-emission SSP1-2.6, and a high-emission scenario SSP5-8.5). Changes in PP were characterized by large regional variability and the response of PP in the sub-polar area was found to differ across the GSR. In SSP5-8.5, a relatively large warming of more than 5°C was found for the Arctic by year 2100, and a significant decrease in winter mixed layer depth of more than 60 m was seen in the sub-polar gyre south of the GSR. Areas north of the GSR showed both a decrease and an increase in MLD, partly due to changes in sea ice cover. The largest change in PP was seen in the sub-polar gyre south of the GSR where PP decreased by up to 20–40 g C m^{-2} yr^{-1} (0.05–0.1 g C m^{-2} d^{-1}), corresponding to a reduction of 10–20% of the PP estimated by the VPP-model for the area (**Table 1**). PP increased north of the GSR, partly due to a decrease in sea ice extent.

A decrease in sub-polar productivity in the ESM-simulations is not in accordance with the less efficient light usage of photosynthesis found here for the area south of the GSR (**Figure 7**). A relatively deep MLD in early spring could explain the relatively low PP during spring and early summer south of the GSR whereas areas north of the GSR were up to 15% more efficient in using light early in the season. Thus, a significant decrease in MLD in this region would likely change the seasonal distribution of PP. A change in PP would require a change in nutrient delivery to surface waters in the region. However, a shallower MLD would increase both the length of time in the productive period when phytoplankton in surface waters are nutrient depleted and also the length of time that nutrients will be regenerated in the surface waters. Thus, we would expect that a shallower MLD would lead to an increase in total PP and not the significant decrease predicted by the multi-model ESM study. This discrepancy between ESM-results and the regional VPP-analysis presented in this study may be explained by other factors included in the ESM-models, i.e., changes in nutrients or grazing. However, the importance of these processes for the PP in the sub-polar area is not well understood and requires further studies.

CONCLUSION

Primary production (PP) between 60 – 70°N in the northern North Atlantic (between Greenland and Norway) was analyzed in two PP-models driven by satellite data and nutrient climatology. The two models (VGPM and VPP) showed consistent results when describing annual PP as well as the seasonal distribution of PP. Analysis by the VPP-model resulted in an annual total PP in the area of 0.46 Pg C yr^{-1}, corresponding to about 1% of the global PP. The averaged areal PP of 0.53 g C yr^{-1} was 43% higher than the global average.

Primary production was averaged in six domains, including parts of the (1) Sub-polar gyre and (2) Nordic Seas, (3) the Southern open shelf south of Iceland and including shelf and shallow areas around the Faroes, (4) Northern open shelf area north of Iceland, (5) Eastern shelf along Greenland, and (6) the Western shelf along Norway. Large regional variability in PP was seen between the six domains where the shelf along east Greenland had the lowest annual PP (0.19 g C m^{-2} d^{-1}) while

the greatest was seen along the Norwegian shelf (0.77 g C m^{-2} d^{-1}). The open shelf areas north and south of the Greenland-Scotland Ridge (GSR) were found to be more productive than the ambient open sea areas.

The average PP during spring, defined from 1 January – 1 June was found to contribute ~25% of the annual PP and the greatest contribution of spring production to total was seen above the Norwegian shelf (34%). In general, variability of PP above the open shelves on either side of the GSR was most highly correlated with PP in the adjacent open seas. This indicates that the dominating influence on the timing of seasonal PP is from water masses, rather than processes related to bathymetry.

Primary production estimates are highly sensitive to the parameterization of the photosynthetic parameter P$^B_{max}$. The parameterization used implies an increase of P$^B_{max}$ during summer due to a higher sea surface temperature (SST). However, comparison with *in situ* measurements of P$^B_{max}$ from the area showed no such dependence on SST. This suggests that PP during the warm period may be overestimated by the parameterization of P$^B_{max}$ applied in the two models. Thus, the PP during summer months may be overestimated here. The general seasonal distribution patterns reported here would, however, remain robust as they are highly dependent on chlorophyll and light distributions.

Areas north of the GSR use light significantly more efficiently for photosynthesis during spring and early summer than in the sub-polar gyre and southern open shelf areas. Thus, light harvesting by phytoplankton in the southern areas first becomes efficient relatively late in the summer season (**Figure 7**). This difference could potentially be explained by nutrient-limitation (e.g., iron and silicate). However, comparison with mixed layer depth (MLD) suggests that deep MLD south of the GSR early in the season is a likely explanation for the less efficient PP compared with the light availability in these areas.

Reduced PP early in the season due to a relatively deep mixed layer implies that PP can potentially increase if MLD decreases significantly. A multi-model ensemble of Earth System Model (ESM) simulations resulted in a significant decrease of MLD and a corresponding decrease of PP by ~10–20% south of the GSR by year 2100 in a warm climate change scenario (SSP5-8.5). A decrease of MLD would imply a significant increase in PP during spring and early summer according to the analysis by the VPP-model. Thus, this discrepancy between regional estimates from a data-driven PP-model and ESM-simulations requires further analysis and indicates a significant uncertainty on the response of PP in the northern North Atlantic to global warming.

DATA AVAILABILITY STATEMENT

Satellite datasets from the Ocean Productivity site were applied for calculation of PP (https://www.science.oregonstate.edu/ocean.productivity) and nitrate data were analyzed from the World Ocean Atlas (Garcia et al., 2010) (https://www.ncei.noaa.gov/products/world-ocean-atlas).

AUTHOR CONTRIBUTIONS

Both authors listed have made a substantial, direct, and intellectual contribution to the work, and approved it for publication.

FUNDING

SUPPLEMENTARY MATERIAL

The Supplementary Material for this article can be found online at: https://www.frontiersin.org/articles/10.3389/fmars.2021.785685/full#supplementary-material

REFERENCES

Arnholt, A. T., and Evans, B. (2021). *BSDA: Basic Statistics and Data Analysis. R package version 1.2.1.*

Astthorsson, O. S., Gislason, A., and Jonsson, S. (2007). Climate variability and the Icelandic marine ecosystem. *Deep Sea Res. II* 54, 2456–2477. doi: 10.1016/j.dsr2.2007.07.030

Behrenfeld, M. J., and Falkowski, P. G. (1997). Photosynthetic rates derived from satellite-based chlorophyll concentration. *Limnol. Oceanogr.* 42, 1–20. doi: 10.4319/lo.1997.42.1.0001

Carr, M.-E., Friedrichs, M. A. M., Schmeltz, M., Aita, M. N., Antoine, D., Arrigo, K. R., et al. (2006). A comparison of global estimates of marine primary production from ocean color. *Deep Sea Res. II* 53, 741–770. doi: 10.1016/j.dsr2.2006.01.028

de Boyer Montégut, C., Madec, G., Fischer, A. S., Lazar, A., and Iudicone, D. (2004). Mixed layer depth over the global ocean: an examination of profile data and a profile-based climatology. *J. Geophys. Res.* 109:C12003. doi: 10.1029/2004JC002378

Debes, H., Gaard, E., and Hansen, B. (2008). Primary production on the Faroe shelf: temporal variability and environmental influences. *J. Mar. Syst.* 74, 686–697. doi: 10.1016/j.jmarsys.2008.07.004

Dugdale, R. C., and Goering, J. J. (1967). Uptake of new and regenerated forms of nitrogen in primary productivity. *Limnol. Oceanogr.* 12, 196–206. doi: 10.4319/lo.1967.12.2.0196

Friedland, K. D., Record, N. R., Asch, R. G., Kristiansen, T., Saba, V. S., Drinkwater, K. F., et al. (2016). Seasonal phytoplankton blooms in the North Atlantic linked to the overwintering strategies of copepods. *Elementa* 4:99. doi: 10.12952/journal.elementa.000099

Garcia, H. E., Locarnini, R. A., Boyer, T. P., Antonov, J. I., Zweng, M. M., Baranova, O. K., et al. (2010). "World Ocean Atlas 2009, Volume 4: nutrients (phosphate, nitrate, silicate)," in *NOAA Atlas NESDIS 71*, ed. S. Levitus (Washington, DC: U.S. Government Printing Office).

Harrison, W. G., Børsheim, K. Y., Li, W. K. W., Maillet, G. L., Pepin, P., Sakshaug, E., et al. (2013). Phytoplankton production and growth regulation in the Subarctic North Atlantic: a comparative study of the Labrador Sea-Labrador/Newfoundland shelves and Barents/Norwegian/Greenland seas and shelves. *Prog. Oceanogr.* 114, 26–45. doi: 10.1016/j.pocean.2013.05.003

Hartmann, D. L. (1994). *Global Physical Climatology.* New York, NY: Academic Press.

Hátún, H., Azetsu-Scott, K., Somavilla, R., Rey, F., Johnson, C., Mathis, M., et al. (2017). The subpolar gyre regulates silicate concentrations in the North Atlantic. *Sci. Rep.* 7:14576. doi: 10.1038/s41598-017-14837-4

Hátún, H., Lohmann, K., Matei, D., Jungclaus, J. H., Pacariz, S., Bersch, M., et al. (2016). An inflated subpolar gyre blows life toward the northeastern Atlantic. *Prog. Oceanogr.* 147, 49–66. doi: 10.1016/j.pocean.2016.07.009

Heezen, B. D., Tharp, M., and Ewing, M. (1959). *The Floors of the Ocean: 1. The North Atlantic, Text to accompany the physiographic diagram of the North Atlantic.* New York, NY: Lamont Geological Observatory.

Henson, S. A., Dunne, J. P., and Sarmiento, J. L. (2009). Decadal variability in North Atlantic phytoplankton blooms. *J. Geophys. Res.* 114:C04013. doi: 10.1029/2008JC005139

Henson, S. A., Sanders, R., Holeton, C., and Allen, J. T. (2006). Timing of nutrient depletion, diatom dominance and a lower-boundary estimate of export production for Irminger Basin, North Atlantic. *Mar. Ecol. Progr. Ser.* 313, 73–84. doi: 10.3354/meps313073

Hillisgøe, K. M., Richardson, K., Bendtsen, J., Sørensen, L. L., Nielsen, T. G., and Lyngsgaard, M. M. (2011). Linking phytoplankton community size composition with temperature, plankton food web structure and sea-air CO2 flux. *Deep Sea Res. I* 58, 826–838. doi: 10.1016/j.dsr.2011.06.004

Holte, J., Talley, L. D., Gilson, J., and Roemmich, D. (2017). An Argo mixed layer climatology and database. *Geophys. Res. Lett.* 44, 5618–5626. doi: 10.1002/2017GL073426

Kwiatkowski, L., Torres, O., Bopp, L., Aumont, O., Chamberlain, M., Christian, J. R., et al. (2020). Twenty-first century ocean warming, acidification, deoxygenation, and upper-ocean nutrient and primary production decline from CMIP6 model projections. *Biogeosciences* 17, 3439–3470. doi: 10.5194/bg-17-3439-2020

Laufkötter, C., Vogt, M., Gruber, N., Aita-Noguchi, M., Aumont, O., Bopp, L., et al. (2015). Drivers and uncertainties of future global marine primary production in marine ecosystem models. *Biogeosciences* 12, 6955–6984. doi: 10.5194/bg-12-6955-2015

Lozier, M., Roussenov, V., Reed, M., and Williams, R. G. (2010). Opposing decadal changes for the North Atlantic meridional overturning circulation. *Nat. Geosci.* 3, 728–734. doi: 10.1038/ngeo947

Lyngsgaard, M. M., Markager, S., Richardson, K., Møller, E. F., and Jakobsen, H. H. (2017). How well does chlorophyll explain the seasonal variation in phytoplankton activity? *Estuar. Coasts* 40, 1263–1275. doi: 10.1007/s12237-017-0215-4

Nielsdóttir, M. C., Moore, C. M., Sanders, R., Hinz, D. J., and Achterberg, E. P. (2009). Iron limitation of the postbloom phytoplankton communities in the Iceland Basin. *Glob. Biogeochem. Cycles* 23:GB3001. doi: 10.1029/2008gb003410

Paris, P. J., Walsh, J. P., and Corbett, D. R. (2016). Where the continent ends. *Geophys. Res. Lett.* 43, 208–212. doi: 10.1002/2016GL071130

Press, W. H., Teukolsky, S. A., Vetterling, W. T., and Flannery, B. P. (1992). *Numerical Recipes in FORTRAN: The Art of Scientific Computing.* Cambridge, MA: Press Syndicate of the University of Cambridge.

R Core Team (2021). *R: A Language and Environment for Statistical Computing.* Vienna: R Foundation for Statistical Computing.

Richardson, K., and Bendtsen, J. (2019). Vertical distribution of phytoplankton and primary production in relation to nutricline depth in the open ocean. *Mar. Ecol. Prog. Ser.* 620, 33–46. doi: 10.3354/meps12960

Richardson, K., Bendtsen, J., Kragh, T., and Mousing, E. A. (2016). Constraining the distribution of photosynthetic parameters in the global ocean. *Front. Mar. Sci.* 3:269. doi: 10.3389/fmars.2016.00269

Ryan-Keogh, T. J., Macey, A. I., Nielsdóttir, M. C., Lucas, M. I., Steigenberger, S. S., Stinchcombe, M. C., et al. (2013). Spatial and temporal development of phytoplankton iron stress in relation to bloom dynamics in the high-latitude North Atlantic Ocean. *Limnol. Oceanogr.* 58, 533–545. doi: 10.4319/LO.2013.58.2.0533

Sanders, R., Brown, L., Henson, S., and Lucas, M. (2005). New production in the Irminger Basin during 2002. *J. Mar. Sys.* 55, 291–310. doi: 10.1016/j.jmarsys.2004.09.002

Skogen, M. D., Budgell, W. P., and Rey, F. (2007). Interannual variability in Nordic seas primary production. *ICES J. Mar. Sci.* 64, 889–898. doi: 10.1093/icesjms/fsm063

Steemann Nielsen, E. (1952). The use of radio-active carbon C14 for measuring organic production in the sea. *ICES J. Mar. Sci.* 18, 117–140. doi: 10.1016/0146-6313(58)90015-7

Sverdrup, H. U. (1953). On conditions for the vernal blooming of phytoplankton. *J. Conseil Conseil Int. Pour l'Exploration Mer* 18, 287–295. doi: 10.1093/icesjms/18.3.287

Takahashi, T., Sutherland, S. C., Sweeney, C., Poisson, A., Metzl, N., Tilbrook, B., et al. (2002). Global sea-air CO2 flux based on climatological surface ocean pCO2, and seasonal biological and temperature effects. *Deep Sea Res.* 49, 1601–1622. doi: 10.1016/S0967-0645(02)00003-6

Takahashi, T., Sutherland, S. C., Wanninkhof, R., Sweeney, C., Feely, R. A., Chipman, D. W., et al. (2009). Climatological mean and decadal change in surface ocean pCO2, and net sea-air CO2 flux over the global oceans. *Deep Sea Res.* 56, 554–577. doi: 10.1016/j.dsr2.2008.12.009

Webb, W. L., Newton, M., and Starr, D. (1974). Carbon dioxide exchange of Alnus rubra. A mathematical model. *Oecologia* 17, 281–291. doi: 10.1007/BF00345747

Zhai, L., Gudmundsson, K., Miller, P. I., Peng, W., Guðfinnsson, H., Debes, H. H., et al. (2012). Phytoplankton phenology and production around Iceland and Faroes. *Cont. Shelf Res.* 37, 15–25. doi: 10.1016/j.csr.2012.01.013